DPU PROCESSING FOR XMM/OM

TRACKING AND COMPRESSION ALGORITHM

DOCUMENT 3

XMM-OM/PENN/TC/0004.03
Author: Cheng Ho
CH6/17/1991

This release of the document "Tracking and Compression Algorithm" (XMM-OM/PENN/TC/0004.03) is to provide an updated discussion on the tracking algorithm. Only chapter 3 of the document is being updated. Chapter 3 of the previous release including figures (XMM-OM/PENN/TC/0004.02) is superceded by this release in its entirety. Changes in this release of Chapter 3 are:

• The original section III.d on Image Quality and related figures are removed. A full discussion on image quality will be presented in a separate document.

• The tracking algorithm has undergone a major overhaul. We have now included the statistical weighting of individual guide stars. The statistical weighting discussion is inserted as III.c. The discussion of the tracking accuracy in III.d is revised accordingly. Furthermore, we have developed two different schemes of handling outlier stars. These are extensively discussed in III.e. These two new developments (statistical weighting and outlier handling) enhance the accuracy of the tracking and also increase the robustness of the algorithm under unfavorable conditions.

III. Tracking

III.a. Basic Formalism

Suppose we have located and chosen N good guide stars within the field of view in the reference frame at (u_i, v_i) where i runs from 1 to N. At a later moment, we take an integration of a frame and determine the new locations of the guide stars at (x_i, y_i). Our task is to determine the change in the aspect of the current frame with respect to the reference frame, i.e. to calculate the drift in the x and y direction as well as the roll with respect to a particular roll center taken to be the origin. The selection of the roll center is *arbitrary*. However, see discussions below on a natural default choice of the roll center where the errors of the calculated drifts are *formally* minimized.

Applying a drift and roll $(\Delta x, \Delta y, \Theta)$ to the guide stars, their new locations are given by

$$\hat{x}_i = u_i C - v_i S + \Delta x \qquad (III.1a)$$

$$\hat{y}_i = u_i S + v_i C + \Delta y, \qquad (III.1b)$$

where $C = \cos\Theta$ and $S = \sin\Theta$. (Without causing any confusion, we use C here for the cosine of the roll angle, while in the rest of this document, C refers to the total count in a stellar image. In III.b., we shall see that the cosine equals to unity for all practical purposes.) With the observed (x_i, y_i), the drifts are calculated by minimizing

$$D^2 = \sum_i w_i D_i^2 \qquad (III.2)$$

where

$$D_i \equiv (x_i - \hat{x}_i)^2 + (y_i - \hat{y}_i)^2, \qquad (III.2a)$$

ans w_i is the statistical weight for the i-th guide star. We shall discuss the assignment of w_i later. For the moment, let's assume that the weight w_i is independent of the drift and roll (Δx, Δy, Θ). Differentiating D^2 with respect to Δx, Δy and Θ at the minimum yields

$$\Delta x = (X - UC + VS)/W \qquad (III.3a)$$

$$\Delta y = (Y - VC - US)/W \qquad (III.3b)$$

$$SP + CQ = 0, \qquad (III.3c)$$

where

$$U = \sum_i w_i u_i, \qquad (III.4a)$$

$$V = \sum_i w_i v_i, \qquad (III.4b)$$

$$X = \sum_i w_i x_i, \qquad (III.4c)$$

$$Y = \sum_i w_i y_i, \qquad (III.4d)$$

$$W = \sum_i w_i, \qquad (III.4e)$$

$$P = \left[\sum_i w_i (x_i u_i + y_i v_i) \right] - (XU + YV)/W, \qquad (III.4f)$$

$$Q = \left[\sum_i w_i (x_i v_i - y_i u_i) \right] - (XV - YU)/W. \qquad (III.4g)$$

For our application, the roll angle is always small and P is always greater than zero, thus the roll angle is given by

$$\Theta = \sin^{-1}(-Q/R) = \sin^{-1}\left[-Q/(P^2 + Q^2)^{1/2}\right]. \qquad (III.5)$$

III.b. Small Roll Angle Approximation

As long as Θ is small, we can make the following approximation in calculating the roll angle,

$$C = 1, \qquad \text{and} \qquad S = \Theta = -Q/R, \qquad (III.6)$$

where

$$R = (Q^2 + P^2)^{-1/2} \simeq P + Q^2/2P. \qquad (III.7)$$

In this small roll angle approximation, calculation of Θ via equation (III.7) does not need the square root operation as in equation (III.5). This approximation will introduce error which is of order Θ^2. Since the roll angle is expected to be on the order of 0.002 radians from the beginning to the end of a 1000-s integration, using equation (III.7) will not introduce any significant error (see below for estimate in the error of Θ).

In summary, the drift and the roll of the satellite are calculated through the equations (III.4) which yields the quantities U, V, X, Y, W, P, and Q. From these quantities, we can calculate the drift and roll in the small angle limit:

$$S = \Theta = -PQ/(P^2 + Q^2/2), \qquad (III.8a)$$

$$\Delta x = (X - U + VS)/W, \qquad (III.8b)$$

$$\Delta y = (Y - V - US)/W. \qquad (III.8c)$$

III.c. Assignment of Statistical Weight

We need to specify the statistical weight in order to carry out the calculation of the drift and roll. The simplest form of the statistical weight is to set w_i uniformly to unity (*uniform weighting*). The calculation is much simplified and this has been the adopted approach in earlier versions of the tracking algorithm. In this case, the uncertainty of the drift and roll is dominated by the worst tracking guide stars, usually the faintest one. Under nominal conditions, there might be a factor of 2 to 3 difference between the brightest and the faintest guide stars. The resulting accuracy is generally acceptable. This could, however, become a problem in a pathological field where the available guide stars are limited and they vary dramatically in brightness. For example, in one particular simulation of a sparse field through a narrow band (1%) filter, the brightest (320 counts/frame) and the faintest (20 counts/s) differ in brightness by a factor of about 16. A uniform statistical weight will then seriously affect the tracking performance. And it is especially in such cases that the tracking accuracy becomes important.

With some increase in processing, we can take into account the varying statistical weights of different guide stars. As discussed in Chapter II of this document, the guide star location algorithm approximately achieve the accuracy of $\sigma_{PSF}/C^{1/2}$ for the centroid of the star, where σ_{PSF} is the standard variation of the detector/system PSF. Thus the statistical weight of individual guide star locations is directly proportional to the counts in the image. Thus, we assign

$$w_i = C_i, \qquad (III.9)$$

where C_i is the count of the guide star image. This quantity is readily available from the guide star location algorithm. For a non-robust (no outlier data point biasing), this is an adequate and simple designation of the statistical weight for the guide stars.

In the actual implementation, we have two choices of incorporating the statistical weight. The first one is to use the counts obtained from the reference frame and apply it throughout (*reference count weighting*). The advantage of this approach is that U, V, W can be pre-calculated before the frame integrations. Some saving in processing could be gained. The disadvantages is that the fluctuation in U, V, W will be frozen. Such fluctuations would be carried over to the frame-by-frame tracking and they could lead to a finite offset in the tracking performance. The second approach is to use the counts for the guide stars in the current frame as the statistical weight (*current count weighting*). While this would be more favorable from the statistical point of view, additional processing would be required.

At the moment, the current count weighting scheme is adopted. CPU timing benchmark is needed to check whether the drift and roll calculation impose a severe processing penalty. If this turn out to be the case, then we would have to consider the reference count weighting scheme.

Figure III.1 shows the tracking result of a nominal situation. Fields with an average stellar density are simulated in white light with random walk drift. The upper left panel shows the distribution of the brightest stars. The upper right panel shows the locations of the guide stars selected by the guide star selection algorithm discussed in Chapter II. The middle left panel shows the deviation between the calculated drift and the (simulated) real drift. The middle right panel shows the same result, only on a finer scale. The lower left panel shows the deviation of the calculated roll from the actual roll. The lower right panel shows the deviation of the observed (from guide star location) guide star locations to the projected (by applying the calculated drift/roll to the reference) guide star locations. In general, the more concentrated the cluster, the better the tracking performance. See discussions below on the application of these quantities for robust outlier handling. Figure III.2 shows the same case as in Figure III.2 except that the stellar density is taken to be in the galactic plane. Figure III.3 shows the case of the galactic pole.

III.d. Precision of the Tracking

Since the observed location of the guide stars (x_i, y_i) as well as the reference locations (u_i, v_i) will no doubt have uncertainties, we expect the calculated drifts and roll to have some uncertainty. We now estimate the errorbar of the tracking quantities and the calculated drift and roll in the case of using the count weighting scheme. We take the error bar for the stellar location in the x and y to be $\delta x_i \simeq \sigma_{PSF}/C_i^{1/2}$. It is straightforward to estimate the standard deviations for X, Y, U, and V:

$$\delta X = \delta Y = \delta U = \delta V = W\langle \delta x \rangle \simeq \sigma_{PSF} W^{1/2}, \qquad (III.10)$$

where $\langle \delta x \rangle = [\sum_i w_i^2 (\delta x_i)^2]^{1/2}/W$. Even though the values of $\delta X(\delta Y)$ and $\delta U(\delta V)$ are the same, we need to make a distinction between them. The quantities U and V are partly universal for the frame-by-frame tracking; errors associated with a linear dependence of them can be easily removed as a systematic error by an after-the-fact calibration to align the star positions with some absolute reference frame; this error is partially reflected in the finite average offset in the tracking performance. linear contributions of U and V in equations (III.8b) and (III.8c) does not affect the precision of the tracking.

The error of Q is

$$\delta Q \simeq \sqrt{R/W} \sigma_{PSF}, \qquad (III.11)$$

and the error of Θ is

$$\delta \Theta \simeq \frac{\delta Q}{R} \simeq \frac{\sigma_{PSF}}{\sqrt{WR}}. \qquad (III.12)$$

The standard deviations for the drifts are

$$\delta(\Delta x) \simeq \frac{\sigma_{PSF}}{\sqrt{W}} \left[1 + \frac{V^2}{WR}\right]^{1/2}, \qquad (III.13a)$$

and

$$\delta(\Delta y) \simeq \frac{\sigma_{PSF}}{\sqrt{W}} \left[1 + \frac{U^2}{WR}\right]^{1/2}. \qquad (III.13b)$$

As long as the roll center is chosen to lie within the field of view, both V^2/WR and U^2/WR will be less than unity.

Mathematically, applying a rotation and translation parameterized by the calculated drift and roll $(\Delta x \pm \delta(\Delta x), \Delta y \pm \delta(\Delta y), \Theta \pm \delta\Theta)$ to any particular point (x, y) point will yield the same result $(x' \pm \delta x', y' \pm y')$, *independent to the choice of the origin (roll center).* However, for efficiency reason, we will only perform on-board compensation to the translation (shift-and-add) to the satellite drift; no compensation will be applied for the roll. The shift-and-add procedure leads to the smallest errorbar at the roll center and the error is greater for points at greater distances from the roll center. Figure III.1 shows the deviation of the calculated drift from the real (simulated) drift. Figure III.2 shows deviation of the calculated roll from the real (simulated) roll. The spread of the deviations is consistent with the estimates given in equations (III.12) and (III.13).

We now discuss a special case where the errorbars of Δx and Δy are *formally* minimized. This is achieved by minimizing U^2 and V^2, i.e., choosing the center-of-mass of the guide stars as the roll center and setting $U = 0$ and $V = 0$. This simplifies equations (8*b*) and (8*c*) to $\Delta x = X/W$ and $\Delta y = Y/W$. The center-of-mass is the natural default roll center. However, with a moderate increase in arithmetics, we shall implementing the tracking algorithm as equation (8) which does leave open the possibility of choosing the roll center at *any* location.

In the simulation for Figure III.1, 10 guide stars are used with an averaged count rate of about 3500 counts/frame, i.e. $W \simeq 35,000$. The estimated (1-sigma) errorbar for $\delta(\Delta x)$ is approximately 0.003 arcsec (with σ_{PSF} of 0.5 arcsec). Visual inspection shows that the calculated fluctuation is slightly worse than this estimate. This is probably the result of finite contribution from the background which is essentially ignored in the discussions above. Similar conclusions is obtained for the cases shown in Figures III.2 and III.3.

III.e. Outlier Handling

In estimating the precision of the tracking calculation [Eqs. (III.12) and (III.13)], we have made the implicit assumption that all guide stars are well-behaved in that they are singular and does not vary with time other than statistical fluctuation. There are, however, situations where this assumption is violated. Such situations include:

- A bad guide star was chosen as a good one in the reference frame due to statistical fluctuation. For example, a binary image may disguise as a good guide star if the fainter stars is particularly weak and the brighter star is particularly strong in the reference frame. Nature, not statistics, could also play cruel trick on us by placing bright yet intrinsically variable stars in our frame. Even with the multiple guide star selection criteria discussed in Chapter II, there is no assurance that only good guide stars will be selected.

- Not enough good guide stars are located in the reference frame. We are forced to use some bad guide stars. Note that we need at least two guide stars to calculate the drift and roll.

• The detector's nonlinearity/nonuniformity could also offset the guide stars' location, even when the guide star itself is well behaved all the way. For example, such distortion could occur at the boundary of the MCP hexagonal pattern.

We have examine two methods of handling the outliers. The first one is detect the outliers and exclude them outright. The second one is to assign smaller weight to the outlier by modifying the weighting factor.

III.e.1. Outlier Exclusion

We begin by examining the guide star consistency through the calculated deviation from equations (III.1) and (III.2). If some of the guide stars turn sour in the tracking frame or a bad guide star was chosen in the reference frame, then these star will have large deviations, i.e., inconsistent with the calculated drift which is dominated by the rest of the presumably well-behaved guide stars. Once we single out the outliers, then excluding it from the drift calculation will enhance the precision of the tracking.

The outlier exclusion algorithm is implemented as follows.

1. We calculate the drift and roll with the current set of guide stars using equations (III.4) to (III.8).

2. We use the calculated drift and roll to calculate the deviation of the observed from the expected locations for individual guide stars. This is done by applying Δx, Δy and Θ (in the small roll angle limit) in equation (III.1) and calculating the deviation for individual guide star D_i^2 defined in equation (III.2).

3. The deviations D_i^2 are sorted by magnitude. The largest deviation $D_{i,\max}^2$ is examined for two outlier exclusion criterions:

$$D_{thld} \text{ exclusion}: \qquad D_{i,\max}^2 > D_{thld}^2, \tag{III.14}$$

or

$$\Omega \text{ exclusion}: \qquad D_{i,\max}^2 > \Omega \times (D^2 - D_{i,\max}^2)/(N_{ggs} - 1), \tag{III.15}$$

where D_{thld}^2 and $\Omega = \omega^2$ are two predetermined parameters for the drift calculation. If either equation (III.14) or (III.15) is satisfied for the outermost guide star, then we've found an outlier and it is excluded from the current guide star list. In each iteration, we only exclude one outlier.

4. With the updated current guide star list, we repeat step 1. The iteration is terminated if no guide star is excluded. Furthermore, to avoid a run-away process where the procedure does not converge, we impose the following additional exit conditions: *a*) the number of excluded guide star should not be greater than a certain number $N_{max,outlier}$, *b*) the number of used guide star should not be less than $N_{min,gs}$. Currently, we use $N_{max,outlier} = 3$ and $N_{min,gs} = 4$.

The key step in the outlier exclusion is equations (III.14) and (III.15). We now discuss the implications of this procedure. The objective of the D_{thld} exclusion is straightforward. The selected D_{thld} is basically an estimate of the largest possible acceptable deviation due to statistics. The theoretical basis of the intuitive Ω exclusion, on the other hand, is more convoluted.

Suppose one of the guide stars turns bad in the current frame, then the Ω exclusion is roughly equivalent to excluding a star which has a deviation such that

$$D_i/\langle D\rangle > N_{ggs}\omega/(N_{ggs}-\omega), \qquad (III.16)$$

where $\langle D\rangle$ is the average deviation we expect from the *good* guide stars. In arriving at equation (III.16) we have taken into account the influence of the bad guide star to the current drift calculation. Several key features in equation (III.16) need to be noted. First, the exclusion is not a linear function of ω; it approximates linear function only when $N_{ggs} \gg \omega$. Second, if $\omega \gtrsim N_{ggs}$, then equation (III.18) cannot be satisfied; the Ω exclusion does not pick up any outlier. In the current implementation, we use $\Omega = 16$. If $N_{ggs} = 10$, then the Ω exclusion is equivalent to a 6-sigma exclusion, if we think of $\langle D\rangle$ as the standard deviation.

In summary, there are four adjustable parameters in the outlier exclusion scheme, D^2_{thld}, Ω, $N_{max,outlier}$ and $N_{min,gs}$. These four numbers should be fine-tuned by extensive simulations and more importantly, applications to realistic data and detector characteristics.

III.e.2. Robust Estimation

The use of robust estimator is well developed. *Numerical Recipe* contains a discussion on the basics of these methods. Here we simply discuss a twist to the robust estimator as in the current implementation.

The idea of robust estimator is to modifying the statistical weighting such that outlier data point will give proportionately smaller contribution. In our current implementation, we modify the statistical weight as (cf. Eq. III.9])

$$W_i' = C_i/(1+\rho C_i D_i^2), \qquad (III.19)$$

where D_i^2 is the deviation calculated through equation (III.2) as discussed in the outlier exclusion algorithm, and ρ is an externally specified parameter.

The essence of the modifier $M_i = (1+\rho C_i D_i^2)^{-1}$ is to simulate the *Lorentzian* distribution. See page 541 of Numerical Recipe for more discussions. Formally, if we assume the underlying distribution is Lorentzian, rather than Gaussian, then the drift and roll are calculated through a set of simultaneous non-linear equation similar to equation (III.4) except that the summations will now include the M_i factor. Since D_i depends on the calculated drift and roll, it is a non-trivial task to find the solution.

In the implementation, we apply an iterative scheme where the calculated drift and roll is fed back into the calculation of the statistical weighting [Eq. (III.18)] in the subsequent iteration. We start the iteration with the non-robust estimation, i.e., setting the weight modifier to unity for the initial iteration. The iteration is terminated after a maximum number of iterations or the improvement in the averaged deviation (D^2/W) becomes negligible.

The meaning of the modifier parameter ρ is the following: Stars whose deviation follows

$$D_i^2 \gtrsim 1/\rho C_i \qquad (III.20)$$

will have a significantly suppressed statistical weight. Compared to the estimate of star location fluctuation $\sigma_{PSF}/C_i^{1/2}$, this means that stars whose deviation is greater than $\sigma_{PSF}/\rho^{1/2}$ standard deviation will be suppressed. In other words, in order to achieve suppression of data points which are k-standard deviation away from expectation, we need to specify ρ as σ_{PSF}/k^2. Currently, we adopt $\rho = 0.05\sigma_{PSF}$ which corresponds to a suppression of point beyond ~ 4.5 standard deviation.

To conclude, we have developed two schemes to handle the possible presence of outliers. The outlier exclusion algorithm applies an abrupt exclusion to eliminate outliers (it's either *in* or *out*), while the robust estimation uses more gradual suppression. The requirement on real-time CPU cycles for these two algorithms appears to be comparable. One can probably identify situations where one algorithm could work better than the other and vice versa. Overall, the robust algorithm has the advantage of having fewer major parameters (ρ versus D_{thld} and Ω), the meaning of this parameter is also more transparent. It is also easier for parameter optimization as the Optical Monitor continues to evolve in the future.

III.f. Summary

In summary, a paradigm has been developed to calculate the satellite drift and roll. There are multiple variations within this paradigm: We can choose among three different weighting factors and we have a choice between two different kinds of outlier handling scheme (plus no outlier handling at all). The decision of which algorithm to use depends on two factors.

First, the algorithm must be efficient enough that the CPU can carry out the calculation without stress. CPU benchmarking/timing is important once the appropriate hardware becomes accessible. Given sufficient CPU power, the current top contender for the tracking algorithm configuration is the iterative robust estimation with current count weighting.

Second, the tracking algorithm must be able to yield acceptable performance over a wide range star fields. The results of tracking with pathological star field is given in a separate document (XMM-OM/PENN/TC/0019.xx). We expect both this document and the compilation of tracking for pathological fields to evolve over the course of this project.

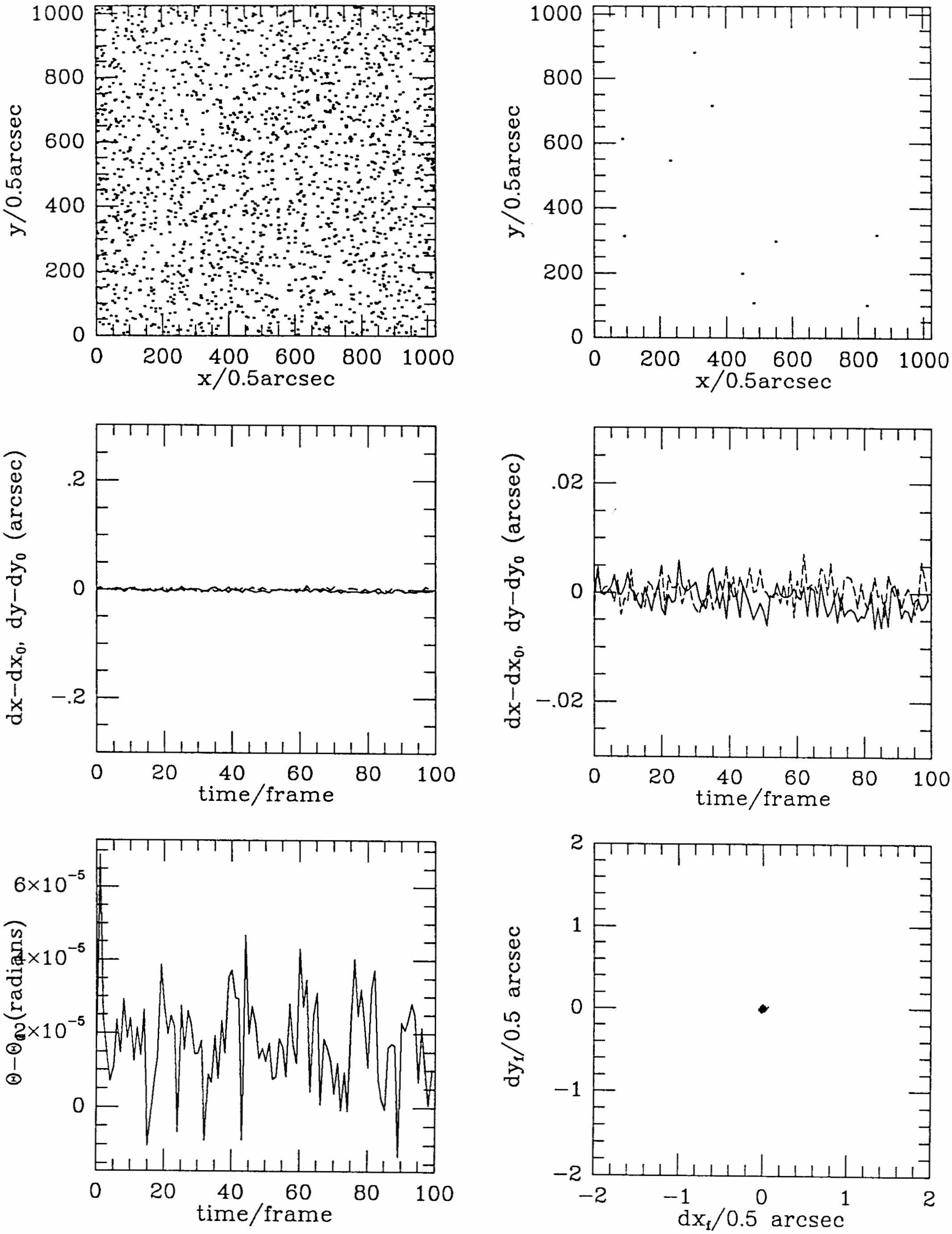

y/0.5arcsec
x/0.5arcsec
dx−dx0, dy−dy0 (arcsec)
time/frame
Θ−Θ0 (radians)
dyf/0.5 arcsec
dxf/0.5 arcsec

Fig. III.2

Figure Captions for Chapter III

Figure III.1 — Tracking performance for an average star field in white light. The upper left panel shows the distribution of the stars. The upper right panel shows the locations of the guide stars selected by the guide star selection algorithm discussed in Chapter II. The middle left panel shows the deviation between the calculated drift and the (simulated) real drift. The middle right panel shows the same result, only on a finer scale. The lower left panel shows the deviation of the calculated roll from the actual roll. The lower right panel shows the deviation of the observed (from guide star location) guide star locations to the projected (by applying the calculated drift/roll to the reference) guide star locations. In general, the more concentrated the cluster, the better the tracking performance. See discussion in III.e on the application of these quantities for robust outlier handling.

Figure III.2 — Same as Figure 1 with a simulated dense (galactic plane) stellar distribution.

Figure III.3 — Same as Figure 1 with a simulated sparse (galactic pole) stellar distribution.

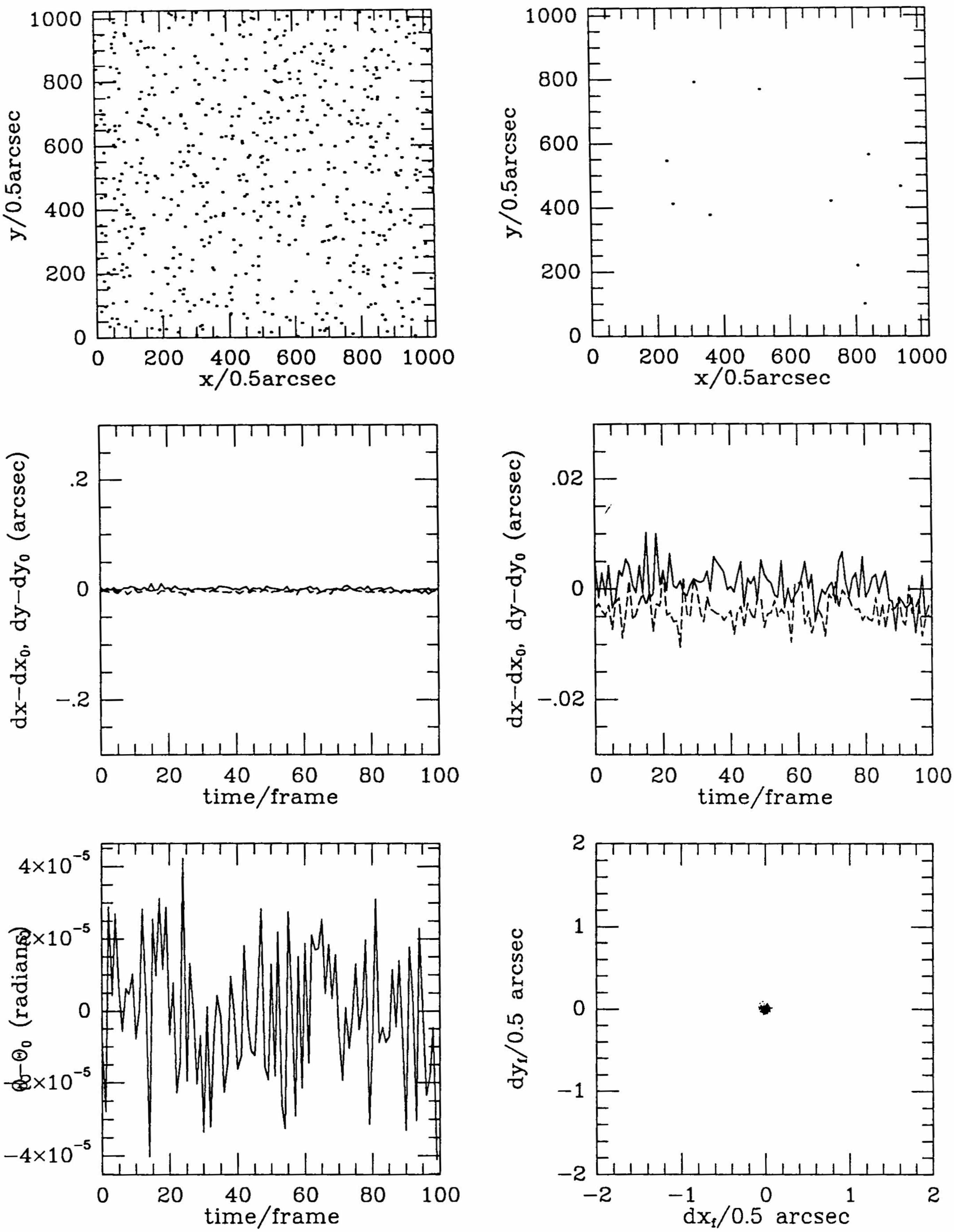

y/0.5arcsec
x/0.5arcsec
dx−dx$_0$, dy−dy$_0$ (arcsec)
time/frame
Θ−Θ$_0$ (radians)
dy$_f$/0.5 arcsec
dx$_f$/0.5 arcsec

Fig. III.1

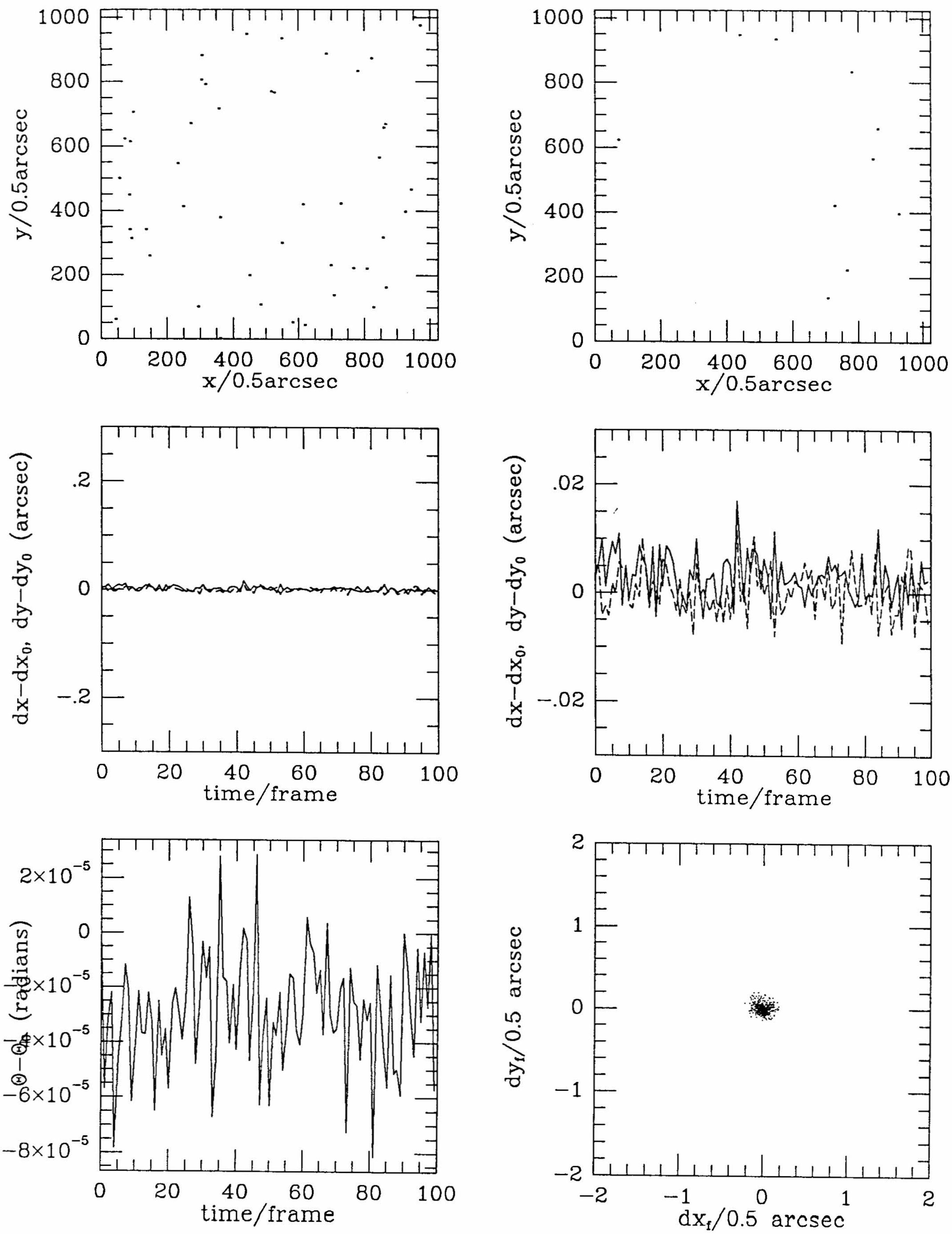
y/0.5arcsec
x/0.5arcsec
y/0.5arcsec
x/0.5arcsec
dx−dx0, dy−dy0 (arcsec)
time/frame
dx−dx0, dy−dy0 (arcsec)
time/frame
Θ−Θ0 (radians)
time/frame
dyf/0.5 arcsec
dxf/0.5 arcsec

Fig. III.3